Inorganic Chemistry
Article

Inorg. Chem. **2009**, *48*, 11779–11787 **11779**
DOI: 10.1021/ic901838r

Neptunium Carbonato Complexes in Aqueous Solution: An Electrochemical, Spectroscopic, and Quantum Chemical Study

Atsushi Ikeda-Ohno,*,†,‡ Satoru Tsushima,† Koichiro Takao,† André Rossberg,† Harald Funke,† Andreas C. Scheinost,† Gert Bernhard,† Tsuyoshi Yaita,‡ and Christoph Hennig*,†

†*Forschungszentrum Dresden-Rossendorf, Institute of Radiochemistry, P.O. Box 510119, 01314 Dresden, Germany and* ‡*Japan Atomic Energy Agency, Synchrotron Radiation Research Center (SPring-8), Kouto 1-1-1, Sayo-cho, Sayo-gun, Hyogo 679-5148, Japan*

Received September 17, 2009

The electrochemical behavior and complex structure of Np carbonato complexes, which are of major concern for the geological disposal of radioactive wastes, have been investigated in aqueous Na_2CO_3 and Na_2CO_3/NaOH solutions at different oxidation states by using cyclic voltammetry, X-ray absorption spectroscopy, and density functional theory calculations. The end-member complexes of penta- and hexavalent Np in 1.5 M Na_2CO_3 with pH = 11.7 have been determined as a transdioxo neptunyl tricarbonato complex, $[NpO_2(CO_3)_3]^{n-}$ ($n = 5$ for Np^V, and 4 for Np^{VI}). Hence, the electrochemical reaction of the $Np^{V/VI}$ redox couple merely results in the shortening/lengthening of bond distances mainly because of the change of the cationic charge of Np, without any structural rearrangement. This explains the observed reversible-like feature on their cyclic voltammograms. In contrast, the electrochemical oxidation of Np^V in a highly basic carbonate solution of 2.0 M Na_2CO_3/1.0 M NaOH (pH > 13) yielded a stable heptavalent Np complex of $[Np^{VII}O_4(OH)_2]^{3-}$, indicating that the oxidation reaction from Np^V to Np^{VII} in the carbonate solution involves a drastic structural rearrangement from the transdioxo configuration to a square-planar-tetraoxo configuration, as well as exchanging the coordinating anions from carbonate ions (CO_3^{2-}) to hydroxide ions (OH^-).

Introduction

The management of radioactive wastes is a critical issue of the nuclear power industry. The geological disposal is one of the possible measures to deal with this knotty problem. International consensus is to dispose of the wastes in underground repositories over a long period of time, to isolate the wastes from the human environment until their radioactivity is sufficiently reduced. A matter of the greatest concern for this waste management strategy is the release of radioactivity from the repository sites through some transport paths before its radioactivity is attenuated enough. The most probable transport process is the dissolution into groundwater, which would erode the engineered barriers and finally release the radionuclides into the geosphere. Hence, understanding the transport property of radionuclides, namely, their migration behavior, in groundwater is the most important subject for assessing the safety and environmental impact of the geological disposal strategy.

Neptunium (Np) is considered to be one of the most problematic nuclides on the geological disposal[1] because it is an α-emitter with a long half-life [e.g., $T_{1/2}(^{237}Np) = 2.14 \times 10^6$ years] and has high solubility under typical groundwater conditions. Groundwater contains various organic and inorganic substances, which potentially interact with the radionuclides including Np. In particular, carbonate species (i.e., carbonate ion (CO_3^{2-}) and hydrogen carbonate ion (HCO_3^-)) are expected to play an important role in the migration behavior of radionuclides on account of their high concentration in groundwater, as well as their strong complexation ability toward various metal ions.[2] Hence, the aqueous Np carbonato complexes are very significant species for the research relevant to the geological disposal of radioactive wastes. As a matter of fact, the thermodynamical properties of Np carbonate species in the aqueous solution system have been extensively investigated by many researchers for the last decades.[3]

The migration behavior of radionuclides is controlled by several physical- and chemical factors. Because the solubility

*To whom correspondence should be addressed. E-mail: a.ikeda-ohno@spring8.or.jp (A.I.-O.), hennig@esrf.fr (C.H.).

(1) Dozol, M.; Hagemann, R. *Pure Appl. Chem.* **1993**, *65*, 1081–1102.

(2) (a) Nash, K. L.; Cleveland, J. M.; Rees, T. F. *J. Environ. Radioact.* **1988**, *7*, 131–157. (b) Clark, D. L.; Hobart, D. E.; Neu, M. P. *Chem. Rev.* **1995**, *95*, 25–48.

(3) (a) Ueno, K.; Saito, A. *Radiochem. Radioanal. Lett.* **1975**, *22*, 127–133. (b) Maya, L. *Inorg. Chem.* **1983**, *22*, 2093–2095. (c) Rai, D.; Ryan, J. L. *Inorg. Chem.* **1985**, *24*, 247–251. (d) Pratopo, M. I.; Moriyama, H.; Higashi, K. *Radiochim. Acta* **1990**, *51*, 27–31. (e) Neck, V.; Runde, W.; Kim, J. I.; Kanellakopulos, B. *Radiochim. Acta* **1994**, *65*, 29–37. (f) Kato, Y.; Kimura, T.; Yoshida, Z.; Nitani, N. *Radiochim. Acta* **1998**, *82*, 63–68. (g) Kitamura, A.; Kohara, Y. *Radiochim. Acta* **2004**, *92*, 583–588.

Published on Web 11/12/2009

of chemical species or their adsorptivity on the surface of natural rocks, which mainly determine the migration behavior, is strongly related to their complex structure, several studies have been performed to elucidate the structural arrangement of aqueous Np carbonate species by Raman,[4] NMR,[5] and X-ray absorption spectroscopies,[5,6] and quantum chemical calculations.[7] All of these prior studies except ref 4 have focused only on the pentavalent neptunium (Np^V) because this oxidation state is expected to be dominant and, thus, the most fundamental under environmentally relevant conditions.[8] As a result, the existing structural information on aqueous Np carbonate species is only for the pentavalent state, and the complex structure with other oxidation states has not yet been unveiled. However, it is well-known that Np can possess five different oxidation states from III to VII in aqueous solution.[9] This means that Np exists not only as the pentavalent state but also potentially occurs with other oxidation states in a natural aquatic environment. Since the complex structure of aqueous Np species is strongly affected by the oxidation state,[10] a comprehensive study should be carried out on the aqueous Np carbonato complexes with different oxidation states to acquire more precise and reliable information for predicting the Np migration behavior on the geological disposal. Especially, Np is expected to exist with higher oxidation states when it migrates to the ground surface or near the surface. This motivates us to perform the present multitechnique study employing electrochemical, spectroscopic (i.e., UV−visible−near-infrared (NIR), infrared (IR), and X-ray absorption), and quantum chemical methods, to elucidate the complex structure of soluble Np carbonato complexes with various oxidation states in aqueous solution. The obtained results are further discussed with the carbonato complexes of other actinides (An).

Experimental Section

Caution! *^{237}Np is a radioactive isotope and an α-emitter. It should be handled in dedicated facilities with appropriate equipment for radioactive materials to avoid health risks caused by radiation exposure.*

Sample Preparation and Electrochemical Experiment. A Np^{VI} stock solution in 1.0 M $HClO_4$ was prepared from neptunium (^{237}Np) dioxide (CEA-Marcoule, France), according to the previously reported procedure.[10b] The radiochemical purity of the stock solution was confirmed by α/γ spectroscopy. All the samples used for electrochemical and spectroscopic experiments were prepared from this stock solution. Electrochemical experiments (i.e., cyclic voltammetry and coulometric electrolysis) were carried out using an Autolab PGSTAT302 potentiostat/galvanostat (Eco Chemie BV). The concentrations and oxidation state of Np in the prepared samples were determined by α/γ spectroscopy and UV−visible−NIR absorption spectroscopy with a Cary 5G UV−visible−NIR spectrophotometer (Varian, Inc.). All of the chemicals (except NpO_2) used in this study were reagent grade and supplied by Merck KGaA and Sigma-Aldrich, Inc.

Np(V) and -(VI) Sample Preparation. The Np^{VI} stock solution was heated to dryness. The dried compound was dissolved in 1.5 M Na_2CO_3 (pH = 11.7), giving a dark yellow solution. The UV−visible−NIR absorption spectrum of this dark yellow solution (shown in Figure S1 in the Supporting Information) exhibited the characteristic peaks of Np^{VI}.[11a,12] Accordingly, this solution was employed as the Np^{VI} sample (sample **2**) in the X-ray absorption experiments. A portion of the Np^{VI} sample solution was also used for preparing the Np^V sample. That is, the Np^{VI} solution was electrolyzed using Pt mesh working- and counter electrodes, and a Ag/AgCl reference electrode (in 3 M NaCl with Vycor glass liquid junction) at −0.15 V (vs Ag/AgCl, the potential values hereafter always refer to Ag/AgCl), according to the voltammetric results given in Figure 3. The resultant solution was almost colorless, and its UV−visible−NIR absorption spectrum was identical with the previously reported spectra of Np^V in aqueous carbonate solutions.[3a,11] This colorless solution was, therefore, employed as the Np^V sample (sample **1**) in the X-ray absorption measurements. The Np concentration in sample **1** (Np^V) was adjusted to be lower than that in sample **2** (Np^{VI}), since the solubility of Np^V in a basic solution is lower than that of Np^{VI}.

Np(VII) Sample Preparation. Precedent studies have suggested that aqueous Np^{VII} species can be stabilized in highly basic solution conditions.[13,14] Hence, the Np^{VII} sample was prepared in a mixed solution of 2.0 M Na_2CO_3 and 1.0 M NaOH (pH > 13) in the following manner: The Np^V solution in 2.0 M Na_2CO_3 (pH = 11.0) was electrochemically prepared from Np^{VI} according to the above-mentioned procedure. An appropriate amount of NaOH pellets was added to the Np^V solution to increase the pH to more than 13. The solution was then electrolyzed at 0.8 V using the same three electrode system used for the Np^V preparation without delay,[15] resulting in the production of a dark green/brown solution. The UV−visible−NIR absorption spectrum of the resultant solution is shown in Figure S1 in the Supporting Information. The

(4) Madic, C.; Hobart, D. E.; Begun, G. M. *Inorg. Chem.* **1983**, *22*, 1494–1503.
(5) Clark, D. L.; Conradson, S. D.; Ekberg, S. A.; Hess, N. J.; Janecky, D. R.; Neu, M. P.; Palmer, P. D.; Tait, C. D. *New J. Chem.* **1996**, *20*, 211–220.
(6) (a) Clark, D. L.; Conradson, S. D.; Ekberg, S. A.; Hess, N. J.; Neu, M. P.; Palmer, P. D.; Runde, W.; Tait, C. D. *J. Am. Chem. Soc.* **1996**, *118*, 2089–2090. (b) Rai, D.; Hess, N. J.; Felmy, A. R.; Moore, D. A.; Yui, M. *Radiochim. Acta* **1999**, *84*, 159–169. (c) Arai, Y.; Moran, P. B.; Honeyman, B. D.; Davis, J. A. *Environ. Sci. Technol.* **2007**, *41*, 3940–3944.
(7) (a) Gagliardi, L.; Roos, B. O. *Inorg. Chem.* **2002**, *41*, 1315–1319. (b) Balasubramanian, K.; Cao, Z. *Inorg. Chem.* **2007**, *46*, 10510–10519.
(8) For instance: (a) Lierse, C.; Treiber, W.; Kim, J. I. *Radiochim. Acta* **1985**, *38*, 27–28. (b) Nitsche, H.; Edelstein, N. M. *Radiochim. Acta* **1985**, *39*, 23–33. (c) Lieser, K. H.; Mühlenweg, U.; Sipos-Galiba, I. *Radiochim. Acta* **1985**, *39*, 35–41.
(9) Yoshida, Z.; Johnson, S. G.; Kimura, T.; Krsul, J. R. In *The Chemistry of the Actinide and Transactinide Elements*, 3rd ed.; Morss, L. R., Edelstein, N. M., Fuger, J., Eds.; Springer: Dordrecht, The Netherlands, 2006; Vol. *2*, p 752.
(10) (a) Antonio, M. R.; Soderholm, L.; Williams, C. W.; Blaudeau, J.-P.; Bursten, B. E. *Radiochim. Acta* **2001**, *89*, 17–25. (b) Ikeda-Ohno, A.; Hennig, C.; Rossberg, A.; Funke, H.; Scheinost, A. C.; Bernhard, G.; Yaita, T. *Inorg. Chem.* **2008**, *47*, 8294–8305. (c) Hennig, C.; Ikeda-Ohno, A.; Tsushima, S.; Scheinost, A. C. *Inorg. Chem.* **2009**, *48*, 5350–5360.
(11) (a) Varlashkin, P. G.; Hobart, D. E.; Begun, G. M.; Peterson, J. R. *Radiochim. Acta* **1984**, *35*, 91–96. (b) Neck, V.; Fanghänel, T.; Kim, J. I. *Radiochim. Acta* **1997**, *77*, 167–175.
(12) (a) Ueno, K.; Hoshi, M. *J. Inorg. Nucl. Chem.* **1971**, *33*, 2631–2633. (b) Pratopo, M. I.; Moriyama, H.; Higashi, K. *J. Nucl. Sci. Technol.* **1993**, *30*, 1024–1029.
(13) (a) Spitsyn, V. I.; Gelman, A. D.; Krot, N. N.; Mefodiyeva, M. P.; Zakharava, F. A.; Komkov, Y. A.; Shilov, V. P.; Smirnova, I. V. *J. Inorg. Nucl. Chem.* **1969**, *31*, 2733–2745. (b) Cohen, D.; Fried, S. *Inorg. Nucl. Chem. Lett.* **1969**, *5*, 653–663. (c) Shilov, V. P.; Stepanova, E. S.; Krot, N. N. *Radiokhimiya* **1976**, *18*, 350–354.
(14) (a) Clark, D. L.; Conradson, S. D.; Neu, M. P.; Palmer, P. D.; Runde, W.; Tait, C. D. *J. Am. Chem. Soc.* **1997**, *119*, 5259–5260. (b) Williams, C. W.; Blaudeau, J.-P.; Sullivan, J. C.; Antonio, M. P.; Bursten, B.; Soderholm, L. *J. Am. Chem. Soc.* **2001**, *123*, 4346–4347. (c) Bolvin, H.; Wahlgren, U.; Moll, H.; Reich, T.; Geipel, G.; Fanghänel, T.; Grenthe, I. *J. Phys. Chem. A* **2001**, *105*, 11441–11445.
(15) Np^V is not stable and hydrolyzed in a basic solution. However, since its hydrolyzation process is relatively slow, we can get a clear Np^V basic solution for several 10 min after adding NaOH. Therefore, the electrolysis from Np^V to Np^{VII} should start right after preparing this "temporary" clear Np^V basic solution. On the other hand, Np^{VI} is more unstable in a basic solution, producing hydroxide precipitates immediately after adding NaOH.

obtained spectrum is in agreement with the reported spectra of Np^{VII} in basic solutions.[11a,13] Hence, this solution was employed as the Np^{VII} sample (sample **3**) in the X-ray absorption and IR experiments. Additionally, another Np^{VI} sample in 2.5 M NaOH was prepared as a reference (sample **4**), according to the reported procedure.[14c]

X-ray Absorption Spectroscopy (XAS). XAS measurements (XANES and EXAFS) were performed on the Rossendorf Beamline (BM20)[16] at the European Synchrotron Radiation Facility (ESRF) under dedicated ring operating conditions (6 GeV, 130−200 mA). A Si(111) double-crystal monochromator was used in channel-cut mode to monochromatize the incoming synchrotron radiation. Higher harmonics were rejected by two Pt-coated mirrors. Np L_{III}-edge absorption spectra were collected in transmission mode using Ar-filled ionization chambers at ambient pressure and temperature. Fluorescence measurement was also performed for a lower Np concentration sample of sample **1** using a 13-element Ge solid state detector (Canberra). Energy calibration of the acquired spectra was carried out by the simultaneous Y K-edge measurement of a reference Y foil (first inflection point at 17 038 eV). The threshold energy, $E_{k=0}$, for Np L_{III}-edge was defined at 17625 eV, regardless of the Np oxidation states. A 0.70−0.75 mL portion of the sample solution was transferred to a triply sealed polystyrene/poly(methyl metacrylate) cuvette (optical path length = 1.0 cm) for XAS measurement. Table 1 summarizes the compositions of the samples used for XAS measurements. At least three scans were performed for each sample, and the spectra were averaged for the data analysis. EXAFS data analysis was performed according to a standard procedure[17] using the program WinXAS (version 3.2).[18] EXAFS structural parameters were calculated by the curve fitting both in the k space (i.e., EXAFS oscillation spectra) and R space (i.e., Fourier-transformed spectra). Theoretical phases and amplitude required for the curve fitting were calculated by FEFF 8.20.[19] All the possible single-scattering (SS) and multiple-scattering (MS) paths were modeled on the basis of the reported crystal structure, $LiNp^{V}O_2CO_3 \cdot 2H_2O$,[20] or the DFT-optimized complex structures. The amplitude reduction factor, ${S_0}^2$, was fixed at 0.9, and the shifts in the threshold energy, $\Delta E_{k=0}$, were constrained to be the same value for all shells on the curve fit procedure.

Infrared (IR) Spectroscopy. Attenuated total reflection Fourier-transform infrared (ATR FT-IR) spectroscopy was performed for the Np^{VII} sample according to the reported procedure and equipment,[21] to acquire supporting information on the unit structure of Np^{VII} species. The data were collected using an ATR flow cell at ambient temperature.

Computational Methods. Density functional theory (DFT) calculations were carried out to optimize the complex structures of possible aqueous Np^{VII} hydroxide/carbonate/hydroxide-carbonate species, as well as to calculate their expected IR spectra. All the calculations were performed in aqueous phase at the B3LYP level without symmetry constraint with the program

Table 1. Summary of XAS Samples

sample ID	oxidation state of Np	[Np]/ M	solvent composition	pH
1	V	0.015	1.5 M Na_2CO_3	11.7
2	VI	0.03	1.5 M Na_2CO_3	11.7
3	VII	0.02	2.0 M Na_2CO_3/1.0 M NaOH	> 13
4	VII	0.015	2.5 M NaOH	> 13

package Gaussian 03.[22] Complex structures were optimized in the aqueous phase using the CPCM solvation model[23] with UAHF radii.[24] The energy-consistent small-core effective core potential (ECP) and the corresponding basis set were employed for neptunium,[25] oxygen,[26] and carbon[26] atoms comprising 60, 10, and 2 electrons in the cores, respectively. Neptunium and oxygen basis sets were supplemented with two g-functions and one d-function, respectively. All the geometry optimizations were followed by vibrational frequency (= IR spectra) analysis to verify the absence of any imaginary frequency in the results.

Results and Discussion

Np(V) and -(VI) Complexes. Figure 1 shows the k^3-weighted Np L_{III}-edge EXAFS spectra (left) and their corresponding Fourier transforms (FTs, right) for Np^{V} and Np^{VI} in 1.5 M Na_2CO_3. Clear EXAFS spectra were acquired until k = 19.6 $Å^{-1}$ both for Np^{V} and Np^{VI}, giving distance resolution, ΔR,[27] of 0.09 Å in the R-space. The observed EXAFS spectra with intricate oscillation patterns produce several significant peaks in their FTs. It is well-known that penta- and hexavalent actinide ($An^{V,VI}$) ions generally form transdioxo cations (i.e., actinyl ions (AnO_2^{n+})) in solution, and that the oxygen atoms of this transdioxo structure (O_{ax}) generate an intense single scattering (SS) peak at around $R + \Delta$ = 1.5 Å ("Δ" represents a phase shift[17]) in EXAFS-FT spectra.[5,6,10] Besides, the linear-arranged transdioxo structure produces a distinguishable multiple scattering[17,28] (MS) peak at around $R + \Delta$ = 2.9 Å.[10b] In addition to these

(16) Matz, W.; Schell, N.; Bernhard, G.; Prokert, F.; Reich, T.; Clauβner, J.; Oehme, W.; Schlenk, R.; Dienel, S.; Funke, H.; Eichhorn, F.; Betzl, M.; Pröhl, D.; Strauch, U.; Hüttig, G.; Krug, H.; Neumann, W.; Brendler, V.; Reichel, P.; Denecke, M. A.; Nitsche, H. *J. Synchrotron Radiat.* **1999**, *6*, 1076–1085.

(17) Prins, R.; Koningsberger, D. E. *X-ray Absorption: Principles, Applications, Techniques for EXAFS, SEXAFS, and XANES*; Wiley-Interscience: New York, 1988.

(18) Ressler, T. *J. Synchrotron Radiat.* **1998**, *5*, 118–122.

(19) Ankudinov, A. L.; Ravel, B.; Rehr, J. J.; Conradson, S. D. *Phys. Rev. B* **1998**, *58*, 7565–7576.

(20) Charushnikova, I. A.; Krot, N. N.; Polyakova, I. N. *Radiokhimiya* **2004**, *46*, 315–317.

(21) (a) Müller, K.; Brendler, V.; Foerstendorf, H. *Inorg. Chem.* **2008**, *47*, 10127–10134. (b) Müller, K.; Foerstendorf, H.; Tsushima, S.; Brendler, V.; Bernhard, G. *J. Phys. Chem. A* **2009**, *113*, 6626–6632.

(22) Frisch, M. J.; Trucks, G. W.; Schlegel, H. B.; Scuseria, G. E.; Robb, M. A.; Cheeseman, J. R.; Montgomery, Jr., J. A.; Vreven, T.; Kudin, K. N.; Burant, J. C.; Millam, J. M.; Iyengar, S. S.; Tomasi, J.; Barone, V.; Mennucci, B.; Cossi, M.; Scalmani, G.; Rega, N.; Petersson, G. A.; Nakatsuji, H.; Hada, M.; Ehara, M.; Toyota, K.; Fukuda, R.; Hasegawa, J.; Ishida, M.; Nakajima, T.; Honda, Y.; Kitao, O.; Nakai, H.; Klene, M.; Li, X.; Knox, J. E.; Hratchian, H. P.; Cross, J. B.; Bakken, V.; Adamo, C.; Jaramillo, J.; Gomperts, R.; Stratmann, R. E.; Yazyev, O.; Austin, A. J.; Cammi, R.; Pomelli, C.; Ochterski, J. W.; Ayala, P. Y.; Morokuma, K.; Voth, G. A.; Salvador, P.; Dannenberg, J. J.; Zakrzewski, V. G.; Dapprich, S.; Daniels, A. D.; Strain, M. C.; Farkas, O.; Malick, D. K.; Rabuck, A. D.; Raghavachari, K.; Foresman, J. B.; Ortiz, J. V.; Cui, Q.; Baboul, A. G.; Clifford, S.; Cioslowski, J.; Stefanov, B. B.; Liu, G.; Liashenko, A.; Piskorz, P.; Komaromi, I.; Martin, R. L.; Fox, D. J.; Keith, T.; Al-Laham, M. A.; Peng, C. Y.; Nanayakkara, A.; Challacombe, M.; Gill, P. M. W.; Johnson, B.; Chen, W.; Wong, M. W.; Gonzalez, C.; and Pople, J. A. *Gaussian 03, Revision D.01*; Gaussian, Inc.: Wallingford, CT, 2004.

(23) Barone, V.; Cossi, M. *J. Phys. Chem. A* **1998**, *102*, 1995–2001.

(24) Bondi, A. *J. Phys. Chem.* **1964**, *68*, 441–451.

(25) Küchle, W.; Dolg, M.; Stoll, H.; Preuss, H. *J. Chem. Phys.* **1994**, *100*, 7535–7542.

(26) Bergner, A.; Dolg, M.; Küchle, W.; Stoll, H.; Preuss, H. *Mol. Phys.* **1993**, *80*, 1431–1441.

(27) The distance resolution, ΔR (Å), is defined as $\Delta R = \pi/2\Delta k$, where Δk ($Å^{-1}$) is the k-range applied for Fourier transformation.

(28) Hudson, E. A.; Allen, P. G.; Terminello, L. J.; Denecke, M. A.; Reich, T. *Phys. Rev. B* **1996**, *54*, 156–165.

(29) Lemire, R. J.; Fuger, J.; Nitsche, H.; Rotter, P.; Rand, M. H.; Rydberg, J.; Spahiu, K.; Sullivan, J. C.; Ullman, W. J.; Vitorge, P.; Wanner, H. *Chemical Thermodynamics of Neptunium and Pltonium*; OECD-NEA, Data Bank Issy-les-Moulineaux, Eds.; OECD-NEA: Amsterdam, The Netherlands, 2001.

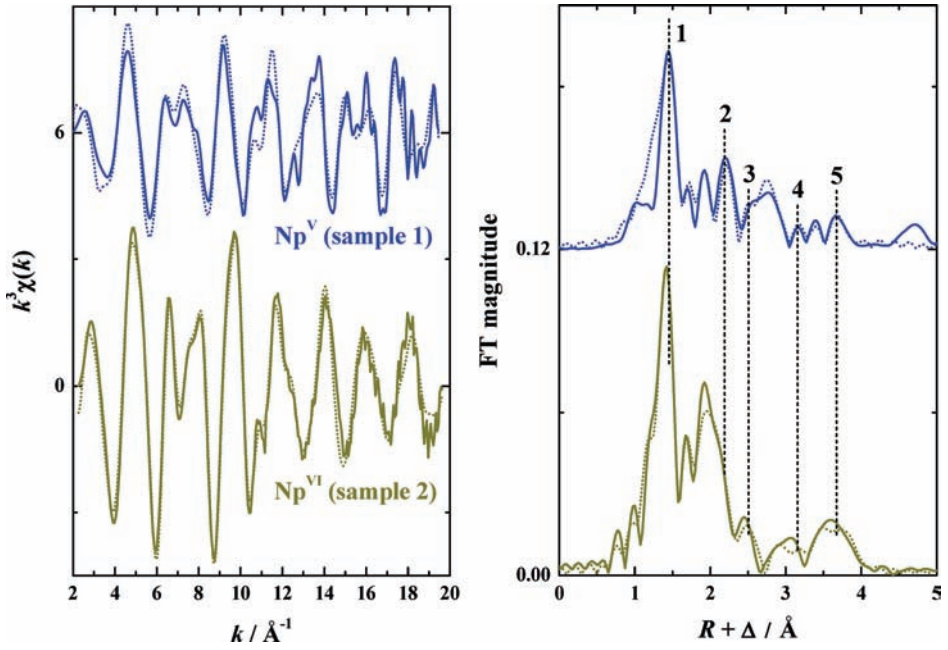

Figure 1. k^3-weighted Np L_{III}-edge EXAFS spectra for Np^V (sample **1**) and Np^{VI} (sample **2**) in 1.5 M Na_2CO_3 at pH = 11.7 (left) and their corresponding Fourier transforms (right): solid line, experimental data; dotted line, theoretical fit; numbers of FT peaks, 1 = O_{ax}−SS, 2 = $O_{eq}(CO_3)$−SS, 3 = $C(CO_3)$−SS, 4 = O_{ax}−MS, 5 = $O_{dist}(CO_3)$ and its MS. Phase shifts are not corrected on the FTs. The data color reflects the actual color of the sample solutions. The FT peaks at $R+\Delta$ = 1.7 and 1.9 Å for Np^V and 1.7 Å for Np^{VI} are artificial peaks, which are produced by the superposition of other strong peaks, and chemically meaningless.[10b]

peaks, three significant peaks are also observed at around $R+\Delta$ = 2.2, 2.5, and 3.6 Å in the present FT spectra. The thermodynamic data[29] suggest that Np^{VI} is expected to form a limiting species of a tricarbonato complex, $[Np^{VI}O_2(CO_3)_3]^{4-}$ in the present solution condition, whereas Np^V predominantly exists as a dicarbonate species. However, Clark and co-workers have revealed that Np^V also forms the tricarbonato complex having a hexagonal bipyramidal arrangement with bidentate carbonate ligation, as illustrated in Figure S2 in the Supporting Information, in aqueous Na_2CO_3 solution.[5,6a] As a matter of fact, the UV−visible−NIR absorption spectrum of the Np^V sample (blue line in Figure S1 in the Supporting Information) agrees with the reported spectra for the tricarbonato complex.[5,6a,11b] Furthermore, we have previously reported that the analogous actinide of uranium (U) also forms the tricarbonato complex, $[UO_2(CO_3)_3]^{n-}$ (n = 5 for U^V, and 4 for U^{VI}), in which three CO_3^{2-} are coordinating to the UO_2^{x+} ion (x = 1 for U^V, and 2 for U^{VI}) with a bidentate fashion, in a similar solution condition.[30] Therefore, the acquired spectra were fitted by assuming a bidentate coordinating tricarbonato complex. The obtained EXAFS structural parameters are summarized in Table 2, along with those reported for U[30] and Pu.[31] The Np^V ion is surrounded by 2 "*yl*" oxygens (O_{ax}) at 1.85 Å and 6 carbonate oxygens ($O_{eq}(CO_3)$), which directly coordinate to the Np ion bidentately, at 2.52 Å in average. The calculated interatomic distances, R, are in good agreement with those reported for the Np^V tricarbonato complex.[5,6a] This also denies the presence of ternary carbonate-hydroxide species, such as $[Np^VO_2(CO_3)_2(OH)]^{3-}$, as a dominant species in the present system, since the strong OH^- coordination should make the average $R(Np^V-O_{eq})$ value shorter than that for the tricarbonato complex. The interatomic distances become shorter as a result of the oxidation from Np^V to Np^{VI}, giving R = 1.79 and 2.45 Å for $Np^{VI}-O_{ax}$ and $Np^{VI}-O_{eq}(CO_3)$ distances, respectively. This shortening can be interpreted mainly by the charge increase of center atom (i.e., Np). Similar change has been observed also for $Np^{V/VI}$ hydrate[10b] and sulfato[10c] complexes, $U^{V/VI}$ carbonato complexes,[30] and $Pu^{V/VI}$ hydrate[32] and carbonato[31b] complexes. On the other hand, a systematic comparison on the $An^{V/VI}$ tricarbonato

Table 2. Summary of EXAFS Structural Parameters of U, Np, and Pu in Aqueous Carbonate Solution

			$_{92}U^b$		$_{93}Np$ (this study)		$_{94}Pu^e$	
oxidation state	shell	scattering path[a]	N	R/Å	N^c	R/Å[d]	N	R/Å
V	O_{ax}	SS	2	1.91	2	1.85	2	1.84
	$O_{eq}(CO_3)$	SS	6	2.50	6	2.52	6	2.50
	C(CO3)	SS	3	2.93	3	2.94		
	$O_{dist}(CO_3)$	SS	3	4.23	3	4.22		
VI	O_{ax}	SS	2	1.81	2	1.79	2	1.75
	$O_{eq}(CO_3)$	SS	6	2.44	6	2.45	6	2.44
	C(CO3)	SS	3	2.92	3	2.90	3	2.89
	$O_{dist}(CO_3)$	SS	3	4.17	3	4.18	3	4.19

[a] SS: single scattering. [b] Reported values in ref 30. [c] Fixed values. [d] Error: $R < \pm 0.01$ Å. [e] Reported values in ref 31.

(30) Ikeda, A.; Hennig, C.; Tsushima, S.; Takao, K.; Ikeda, Y.; Scheinost, A. C.; Bernhard, G. *Inorg. Chem.* **2007**, *46*, 4212–4219 (Corrections: **2009**, *48*, 6321).
(31) (a) Clark, D. L. *Los Alamos Science* **2000**, *26*, 364–381. (b) Conradson, S. D.; Abney, K. D.; Begg, B. D.; Brady, E. D.; Clark, D. L.; den Auwer, C.; Ding, M.; Dorhout, P. K.; Espinosa-Faller, F. J.; Godron, P. L.; Haire, R. G.; Hess, N. J.; Hess, R. F.; Keogh, D. W.; Lander, G. H.; Lupinetti, A. J.; Morales, L. A.; Neu, M. P.; Palmer, P. D.; Paviet-Hartmann, P.; Reilly, S. D.; Runde, W. H.; Tait, C. D.; Veirs, D. K.; Wastin, F. *Inorg. Chem.* **2004**, *43*, 116–131.
(32) (a) Conradson, S. D. *Appl. Spectrosc.* **1998**, *52*, 252A–279A. (b) Ankudinov, A. L.; Conradson, S. D.; de Leon, J. M.; Rehr, J. J. *Phys. Rev. B* **1998**, *57*, 7518–7525.

complex series suggests that, in the same oxidation state, the bond distance for actinyl oxygens (R(An−O_{ax})) becomes shorter across the An series, while the distances related to the carbonate coordination are quite similar. It is well-known that the ionic radii of An ions decrease with increasing atomic number because of the actinide contraction.[33] Assuming that the observed shortening of the An−O_{ax} distance simply originates in the decrease of $An^{V/VI}$ ionic radii by the actinide contraction, the An−O_{ax} distances are expected to show a monotonic and linear decrease, as drawn as dotted lines in Figure 2.[34] However, the observed An−O_{ax} distances obviously deviate downward from these dotted lines, implying that the shortening of the An−O_{ax} distance is caused not only by the actinide contraction but also by other factors. One possible factor is the participation of f-electrons in actinyl bonding. It has been reported that the presence of f-electrons possibly enhances the actinyl bond strength by forming 6p-5f hybrid orbitals.[35] Hence, the increase of f-electrons may lead to the further shortening of An−O_{ax} distance. In particular, one f-electron increase from $[Rn]f^1$ to $[Rn]f^2$ (i.e., $U^V \rightarrow Np^V$ and $Np^{VI} \rightarrow Pu^{VI}$) results in a significant decrease in An−O_{ax} distance, implying that this electron configuration change may involve a considerable change in the An−O_{ax} bond property. On the other hand, the bond distances of CO_3^{2-} on the equatorial plane are almost unchanged, regardless of atomic number. This indicates that f-electrons play less significant role in forming chemical bonds on the equatorial plane and, consequently, An−$O_{eq}(CO_3)$ distances simply depend on the charge of the actinyl center. It should be noted that the FT peak at around $R + \Delta = 2.0$ Å in the Np^{VI} spectrum appears to consist of two components. As a matter of fact, the curve fitting for this peak with two different $O_{eq}(CO_3)$ shells calculates 3 $O_{eq}(CO_3)$ at 2.40 Å and 3 other $O_{eq}(CO_3)$ at 2.50 Å, within the ΔR value of 0.09 Å. In general, the carbonate coordination to An ions exhibits a symmetric bidentate arrangement both in solid crystals[20,36] and in solution.[30,36c] However, some sodium pentacarbonato complexes of Th^{IV} [37a] and Ce^{IV} [37b], $Na_6[M^{IV}(CO_3)_5]\cdot 12H_2O$, display an asymmetric carbonate ligation. This asymmetric arrangement can be interpreted as a result of the interaction with the counter cations (Na^+) in the outer coordination sphere.[38] The present carbonate solution (1.5 M Na_2CO_3) contains a considerable amount of Na^+, which possibly interacts with the highly anionic $[Np^{VI}O_2(CO_3)_3]^{4-}$ complex. However, since there is still little comparable information available on Np^{VI} carbonate species, further investigation is required to draw a conclusion of this asymmetric carbonate ligation in the present Np^{VI} complex.

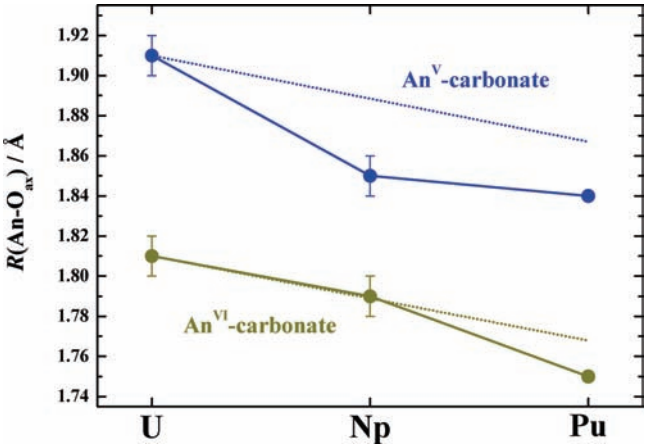

Figure 2. An−O_{ax} bond distances in An^V- and An^{VI} tricarbonato complexes. The U and Pu data are taken from refs 30 and 31b, respectively (errors are not reported for the Pu data). The dotted lines are calculated from the ionic radii reported by Shannon. See the text.

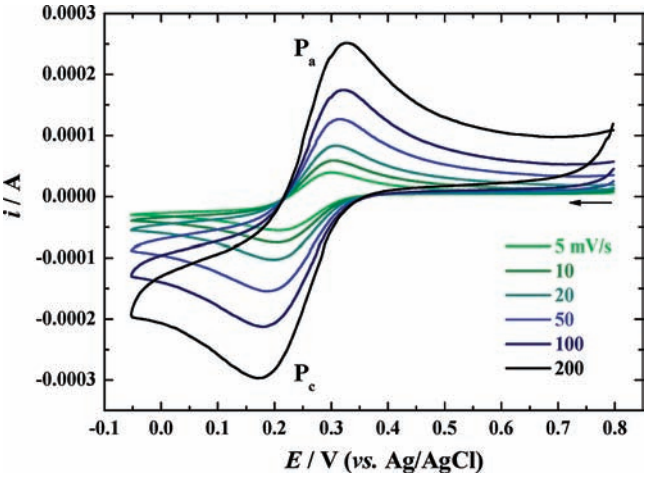

Figure 3. Cyclic voltammograms of 0.01 M Np^{VI} in 1.5 M Na_2CO_3 at pH = 11.8: working electrode, Pt (surface area = 2.01 mm^2); initial scan direction, cathodic from 0.8 V.

Figure 3 shows the cyclic voltammograms (CVs) of Np^{VI} in 1.5 M Na_2CO_3 at pH = 11.8. A pair of cathodic (P_c) and anodic (P_a) peaks was observed in each CV. The peak separation between P_c and P_a becomes slightly wider with increasing scan rate. These results indicate that the observed electrochemical reaction is neither reversible nor irreversible, but it is categorized in a quasi-reversible reaction.[39] The EXAFS results suggest that both Np^V and Np^{VI} form the same neptunyl tricarbonato complex in 1.5 M Na_2CO_3, meaning that the redox reaction between Np^V and Np^{VI} is a simple one-electron reaction without involving structural rearrangement. It has been reported that the electrochemical reaction of the analogous redox couple of U^V and U^{VI}, which also form the structurally identical uranyl tricarbonato complex, proceeds quasi-reversibly.[30] As compared with the large peak separation (0.4−0.5 V) observed for the U^V/U^{VI} redox couple, the

(33) Edelstein, N. M.; Fuger, J.; Katz, J. J.; Morss, L. R. In *The Chemistry of the Actinide and Transactinide Elements*, 3rd ed.; Morss, L. R., Edelstein, N. M., Fuger, J., Eds.; Springer: Dordrecht, The Netherlands, 2006; Vol. *3*, p 1798.

(34) The dotted lines in Figure 2 are calculated from the ionic radii reported by Shannon: Shannon, R. D. *Acta Crystallogr.* **1976**, *A32*, 751–767; The detailed calculation procedure is described in Supporting Information.

(35) Denning, R. G. *Struct. Bonding* (*Berlin*) **1992**, *79*, 215–276.

(36) (a) Coda, A.; Giusta, A. D.; Tazzoli, V. *Acta Crystallogr. B* **1981**, *37*, 1496–1550. (b) Mereiter, K. *Acta Crystallogr. C* **1986**, *42*, 1682–1684. (c) Clark, D. L.; Conradson, S. D.; Keogh, D. W.; Palmer, P. D.; Scott, B. L.; Tait, C. D. *Inorg. Chem.* **1998**, *37*, 2893–2899.

(37) (a) Voliotis, S.; Rimsky, A. *Acta Crystallogr.* **1975**, *B31*, 2615–2620. (b) Voliotis, S.; Rimsky, A. *Acta Crystallogr.* **1975**, *B31*, 2620–2622.

(38) Tsushima, S.; Uchida, Y.; Reich, T. *Chem. Phys. Lett.* **2002**, *357*, 73–77.

(39) Bard, A. J.; Faulkner, L. R. In *Electrochemical Methods: Fundamentals and Applications*, 2nd ed.; John Wiley and Sons, Inc.: New York, 2001.

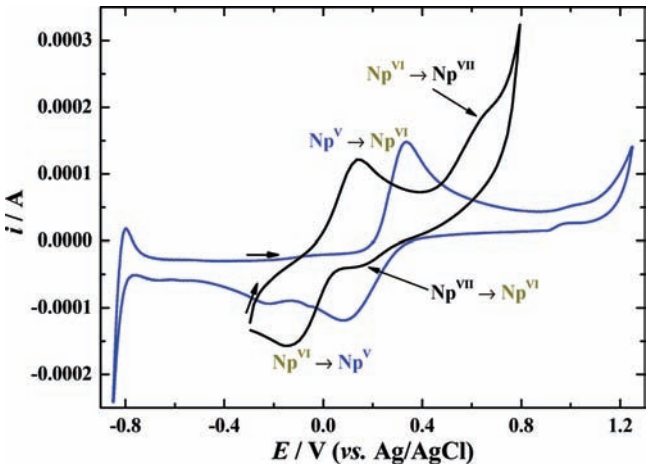

Figure 4. Cyclic voltammograms of 0.01 M Np^{V} in Na_2CO_3 with different pH: blue line, 2.0 M Na_2CO_3 at pH = 11.0; black line, 2.0 M Na_2CO_3/1.0 M NaOH at pH > 13; working electrode, Pt (surface area = 2.01 mm^2); initial scan direction, anodic from 0.3 V. A small cathodic peak at −0.25 V in the blue line corresponds to the H^+ adsorption on the electrode surface.

Np^{V}/Np^{VI} redox couple shows much smaller peak separation (0.1−0.2 V). This suggests that, although both reactions are categorized as quasi-reversible, the reaction kinetics for the Np^{V}/Np^{VI} redox couple inclines toward reversible, while that for the U^{V}/U^{VI} couple is rather irreversible-like. As shown in Figure 2, the reduction from Np^{VI} to Np^{V} involves less An−O_{ax} bond lengthening (3.3%) than that from U^{VI} to U^{V} (5.5%), indicating that the structural rearrangement in the $Np^{V/VI}$ redox reaction is gentler than that for the $U^{V/VI}$ redox couple. This might be the reason for the observed reversible-like feature of the Np^{V}/Np^{VI} redox couple.

Np(VII) Complex. One of the interesting features of Np chemistry is the possibility to reach the heptavalent state, Np^{VII}. Preceding studies[13,14] suggest that Np^{VII} tends to be stabilized in a highly basic solution. Figure 4 shows the CVs of Np^{V} in Na_2CO_3 at different pH. The CV at pH = 11.0 (the blue line in Figure 4) displays only one pair of redox peaks at 0.3 and 0.1 V, corresponding to the redox reaction between Np^{V} and Np^{VI}, within the scanned range from −0.85 to 1.25 V. As the pH is increased, these peaks are shifted to lower potential. Furthermore, in addition to these redox peaks, one more pair of small but distinguishable peaks appears at 0.6 and 0.2 V on the CV at pH > 13 (the dark-green line in Figure 4). The potential values of these additional peaks are analogous to those reported for the Np^{VI}/Np^{VII} couple in a concentrated LiOH solution,[40] suggesting that the observed additional peaks are probably related to the redox reaction between Np^{VI} and Np^{VII}. As a matter of fact, the electrolysis of Np^{V} at 0.8 V in the same Na_2CO_3 solution with pH > 13 resulted in the production of a dark green/brown solution, whose UV−visible−NIR absorption spectrum (shown in Figure S1 in the Supporting Information) is identical to that reported for Np^{VII}.[11a,13] Hence, we conclude that the additional peaks observed at 0.6 and 0.2 V are attributed to the redox reaction between Np^{VI} and Np^{VII}. It should be noted that the Np^{V} and Np^{VI} species dissolved in the 2.0 M Na_2CO_3/1.0 M NaOH solution probably form the tricarbonato complex, $[NpO_2(CO_3)_3]^{n-}$ (n = 5 for Np^{V} and 4 for Np^{VI}), since the hydroxo- or binary hydroxo-carbonato complexes of Np^{V} and Np^{VI} are expected to have very low solubility in the present high pH region.[29]

The k^3-weighted EXAFS spectrum for the prepared Np^{VII} sample (sample **3**) and its corresponding FT are shown in Figure 5, along with those for the reference sample of Np^{VII} in 2.5 M NaOH (sample **4**). Both samples exhibit a single component-like oscillation pattern, producing an intense peak at $R + \Delta$ = 1.5 Å and a small peak at $R + \Delta$ = 1.9 Å on their FTs. Several EXAFS and quantum chemical studies,[14b,c] as well as an NMR study,[41] have revealed that, in a concentrated NaOH solution, Np^{VII} forms a tetraoxo dihydroxo complex, $[Np^{VII}O_4(OH)_2]^{3-}$ (Structure **C** in Figure 7). In addition to the coordination of hydroxide ions (OH^-), CO_3^{2-} can possibly coordinate to Np^{VII} in the present Na_2CO_3/NaOH mixed solution, since CO_3^{2-} is known as an exceptionally strong ligand for An as well as OH^-. As a matter of fact, several carbonate-hydroxide binary complexes have been reported for Np^{IV}, Np^{V}, and Np^{VI}.[29] Hence, DFT structural optimization was performed for several Np^{VII} complexes, which conceivably form in the present Na_2CO_3/NaOH mixed solution, to find the most consistent structure for the obtained EXAFS data. The optimized complexes are illustrated in Figure 7, and their calculated bond distances are summarized in Table 3.

Structures **A** and **B** in Figure 7 represent the trans-dioxo and trioxo Np^{VII} complexes, respectively. The optimized structures of these complexes have bidentate-coordinating CO_3^{2-}, which are supposed to exhibit a strong SS peak attributed to the coordinating oxygen atoms ($O_{cood}(CO_3)$) on the EXAFS-FT spectrum at around $R + \Delta$ = 2.0 Å. The obtained FT spectrum in Figure 5 shows, however, only a small peak at 1.9 Å. Besides, as demonstrated in Figure 6, the Np L_{III}-edge XANES spectrum, which is sensitive to the structural arrangement of actinyl moieties,[28,42] of sample **3** exhibits a completely different shape as compared to that for the *trans*-dioxo Np^{V} (sample **1**) or Np^{VI} (sample **2**) complex, but rather analogous to the spectrum reported for the square-planar-tetraoxo Np^{VII} complex (= sample **4**).[14b,c]

The present DFT calculations also involve the generation of the IR spectrum for each optimized complex. The computed IR spectra for the complexes in Figure 7 are given in the Supporting Information (Figures S10−S14). These IR spectra suggest that all the tetraoxo complexes (i.e., Structures **C**, **D**, and **E**) display intense peaks related to their asymmetric stretching vibrational mode (ν_3) at around 700−750 cm^{-1} (Figures S12−S14, Supporting Information), while the ν_3 vibrational frequencies of the dioxo (Structure **A**, Figure S10, Supporting Information) and trioxo (Structure **B**, Figure S11, Supporting Information) complexes appear at 960 and 860 cm^{-1}, respectively. The ATR FT-IR spectrum of sample **3** (Figure S15 in the Supporting Information) shows,

(40) Gelis, A. V.; Vanysek, P.; Jensen, M. P.; Nash, K. L. *Radiochim. Acta* **2001**, *89*, 565–571.

(41) Appelman, E. H.; Kostka, A. G.; Sullivan, J. C. *Inorg. Chem.* **1988**, *27*, 2002–2005.

(42) Denecke, M. A.; Dardenne, K.; Marquardt, C. M. *Talanta* **2005**, *65*, 1008–1014.

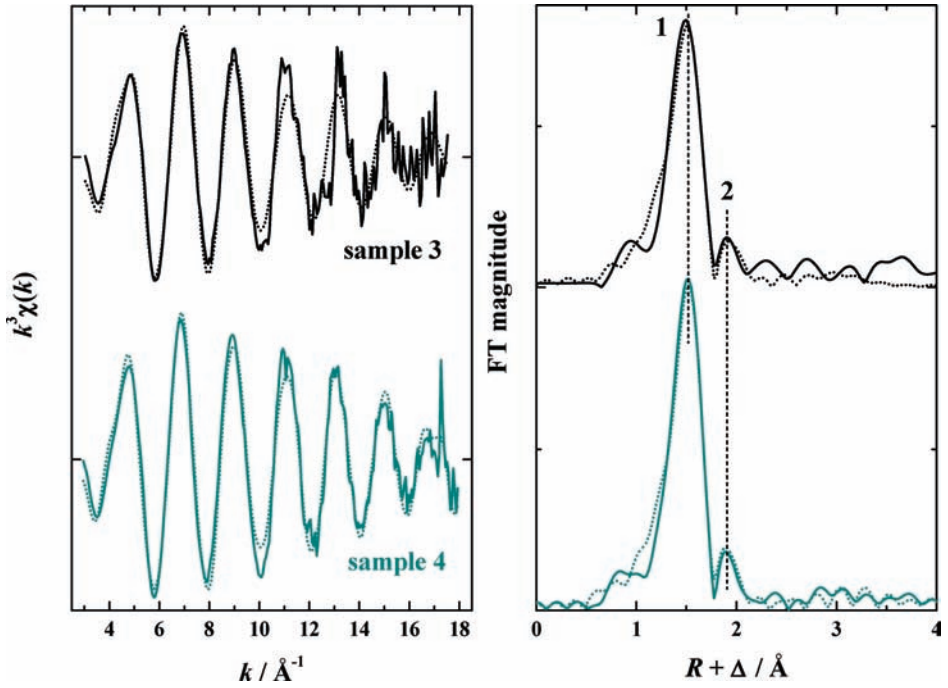

Figure 5. k^3-weighted Np L_{III}-edge EXAFS spectra (left) for Np^{VII} in 2.0 M Na_2CO_3/1.0 M NaOH (upper black data, sample **3** in Table 1) and in 2.5 M NaOH (lower cyan data, sample **4** in Table 1) and their corresponding Fourier transforms (right): solid line, experimental data; dotted line, theoretical fit; numbers of FT peaks, 1 = O_{oxo}−SS, 2 = O(OH)−SS. Phase shifts are not corrected on the FTs.

however, no significant peak above 800 cm^{-1}. Besides, it was difficult to acquire a meaningful spectrum below 800 cm^{-1} because of the strong absorption of water. Taken together, we conclude that the tetraoxo structure is the most probable arrangement for the Np^{VII} unit in 2.0 M Na_2CO_3/1.0 M NaOH. The XANES spectrum in Figure 6 also supports this conclusion. That is, the XANES of $Np^{V}O_2^{+}$ and $Np^{VI}O_2^{2+}$ show a MS feature at around 17630 eV, which results from the interference of the transdioxo moiety.[19,42] The Np^{VII} sample exhibits a further enhanced MS peak, giving a clear hint toward an increasing number of the oxo groups. This is also supported by several theoretical studies,[14b,c,43] proposing that the square-planar-tetraoxo arrangement is the most appropriate for Np^{VII} than others.

As already mentioned, Structure **C** ($[Np^{VII}O_4(OH)_2]^{3-}$) is expected to be formed in a concentrated NaOH solution, like 2.5 M NaOH (i.e., sample **4**). Therefore, the EXAFS curve fit for sample **4** was performed by assuming Structure **C**. The obtained structural parameters listed in Table 4 are consistent with the reported values of $R(Np-O_{oxo})$ = 1.87 Å and $R(Np-O(OH))$ = 2.24 Å,[14b] or $R(Np-O_{oxo})$ = 1.89 Å and $R(Np-O(OH))$ = 2.32 Å.[14c] These values are also in good agreement with the reported crystal structure of the analogous Pu^{VII} complex, $[Pu^{VII}O_4(OH)_2]^{3-}$.[44] As given in Table 3, the DFT-optimized bond distances for Structure **C** are in good agreement with these EXAFS results, for example, we obtain the $R(Np-O_{oxo})$ value of 1.89 Å by EXAFS, while the DFT-optimized complex has an average $Np-O_{oxo}$ distance of 1.893 Å. This indicates that the bond distances (especially

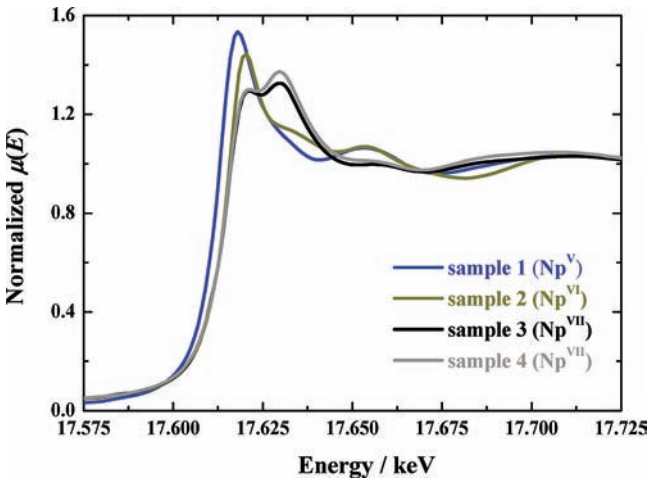

Figure 6. Np L_{III}-edge XANES spectra for Np^{V} (sample **1**) and Np^{VI} (sample **2**) in 1.5 M Na_2CO_3, and Np^{VII} in 2.0 M Na_2CO_3/1.0 M NaOH (sample **3**) and in 2.5 M NaOH (sample **4**).

$R(Np-O_{oxo})$ values) obtained from the present DFT calculations are fairly reliable. Structures **D** and **E** have one and two CO_3^{2-} at the apexes of the tetragonal pyramid with the tetraoxo plane base, respectively. These CO_3^{2-} coordinate to the Np^{VII} ion in a unidentate fashion because of the limited coordination space, differing from the dioxo and trioxo complexes having the bidentate coordinating CO_3^{2-}. The $Np-O_{oxo}$ distances for the optimized tetraoxo complexes are almost unchanged (1.88−1.89 Å), regardless of the type of coordinating anions. On the other hand, there is a considerable difference in bond distance between the OH^- and CO_3^{2-} ligations. That is, the $Np-O_{cood}(CO_3)$ distance (2.46−2.48 Å) is approximately 0.1 Å longer than the Np−O(OH) distance (2.38−2.39 Å). This means that, if the Np^{VII} species in sample **3** forms a carbonato complex, its

(43) (a) Bolvin, H.; Wahlgren, U.; Gropen, O.; Marsden, C. *J. Phys. Chem. A* **2001**, *105*, 10570–10576. (b) Wren, J. E. C.; Schreckenbach, G. *Can. J. Chem.* **2009**, *87*, 1436−1443.

(44) Grigoriev, M. S.; Krot, N. N. *Acta Crystallogr.* **2007**, *E63*, i108–i110.

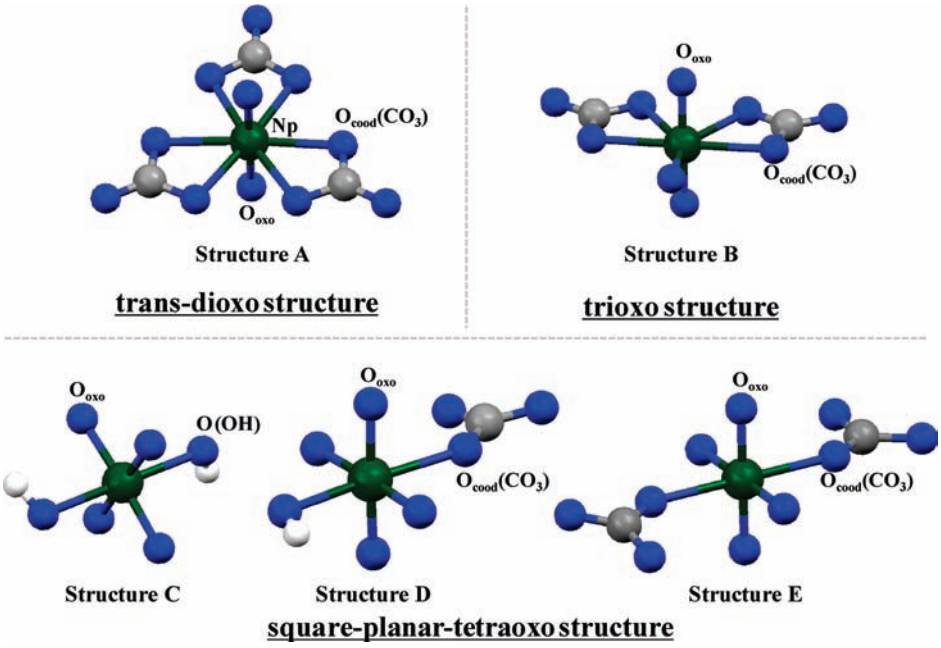

Figure 7. DFT-optimized structures of Np^{VII} carbonato/hydroxo complexes at the B3LYP level in aqueous solution. The calculated bond distances are given in Table 3.

Table 3. Average Interatomic Distances of Np^{VII} Complexes Optimized at the B3LYP Level in Aqueous Solution

complex	ID in Figure 7	Np−O_{oxo}	bond distance/Å Np−O(OH)	Np−$O_{cood}(CO_3)$
$[NpO_2(CO_3)_3]^{3-}$	Structure A	1.755		2.380
$[NpO_3(CO_3)_2]^{3-}$	Structure B	1.825		2.421
$[NpO_4(OH)_2]^{3-}$	Structure C	1.893	2.391	
$[NpO_4(CO_3)(OH)]^{4-}$	Structure D	1.883	2.380	2.480
$[NpO_4(CO_3)_2]^{5-}$	Structure E	1.875		2.463

Table 4. Summary of EXAFS Structural Parameters for Np^{VII} Samples

sample ID	solvent	shell	scattering path[a]	N^b	R/Å[c]
3	2.0 M Na_2CO_3/1.0 M NaOH	O_{oxo}	SS	3.9	1.89
		O(OH)	SS	2.3	2.33
4	2.5 M NaOH	O_{oxo}	SS	4.0	1.89
		O(OH)	SS	2.4	2.35

[a] SS: single scattering. [b] Error: $N < \pm 10\%$. [c] Error: $R < \pm 0.01$ Å.

corresponding EXAFS-FT peak (i.e., Peak 2 in Figure 5) should shift to a longer R range. However, the position of Peak 2 for sample **3** is almost identical with that for sample **4**. Considering these facts, we conclude that the Np^{VII} species formed in sample **3** is most likely to be the tetraoxo dihydroxo complex, $[Np^{VII}O_4(OH)_2]^{3-}$, which is identical to the reported Np^{VII} complex in a concentrated NaOH solution. Accordingly, the EXAFS curve fit for sample **3** was carried out by assuming the tetraoxo dihydroxo complex structure. The obtained structural parameters are summarized in Table 4. The calculated coordination numbers (N) and R for sample **3** are in good agreement with those for sample **4**, and are consistent with the tetraoxo dihydroxo complex. These results also support the above conclusion that Np^{VII} forms $[Np^{VII}O_4(OH)_2]^{3-}$ even in the present carbonate solution.

On the basis of the above-mentioned experimental results and conclusions, we can briefly summarize the chemical features of Np^{VII} in Na_2CO_3 solutions: (1) the electrochemical oxidation from $Np^{V/VI}$ to Np^{VII} involves a drastic structural rearrangement from the *trans*-dioxo $[NpO_2(CO_3)_3]^{n-}$ complexes to the square-planar-tetraoxo $[Np^{VII}O_4(OH)_2]^{3-}$ complex, (2) the tetraoxo structure seems to be required to stabilize the heptavalent state in an aqueous alkaline solution, (3) the OH^- coordination overcomes the strong CO_3^{2-} coordination even in a concentrated carbonate solution, (4) the hydroxo Np^{VII} complex, $[Np^{VII}O_4(OH)_2]^{3-}$, is soluble in aqueous solution and its solubility is relatively high. Summary feature (1) rationalizes the observed large CV peak separation for the $Np^{VI/VII}$ redox couple in Figure 4. In connection with Summary feature (3), one may wonder why the carbonate coordination is inhibited, despite its strong coordination ability. The interpretation of this phenomenon seems to be rather simple. Contrary to the positively charged *trans*-dioxo NpO_2^{n+} unit, the square-planar-tetraoxo $Np^{VII}O_4^-$ unit is negatively charged. Accordingly, its interaction with anionic CO_3^{2-} ought to be weak, so that the carbonate coordination cannot compete with the hydroxo coordination. Besides, as compared to the trans-dioxo structure, the square-planar-tetraoxo structure has a strict limitation on its coordination space, allowing CO_3^{2-} to coordinate only with the unidentate mode. It is obvious from the bond distances calculated by DFT that the unidentate coordinating CO_3^{2-} is much weaker than the bidentate coordinating one. Summary feature (4) might be a potential concern for the assessment of Np migration on the ground surface/near the surface or

in the pore water of vitrified radioactive wastes, although highly basic and oxidizing conditions are less probable in such environments.

Conclusions

In this study, we have performed the electrochemical and structural studies on the limiting carbonate species of Np with different oxidation states in an aqueous solution by means of cyclic voltammetry, X-ray absorption spectroscopy, and DFT calculations. The penta- and hexavalent Np form the limiting complex of $[NpO_2(CO_3)_3]^{n-}$ (n = 5 for Np^V, and 4 for Np^{VI}) in 1.5 M Na_2CO_3 with pH = 11.7, meaning that their redox reaction proceeds as a simple one-electron reaction without any structural rearrangement. These electrochemical and complexation properties of $Np^{V/VI}$ are quite similar to their analogous An of $U^{V/VI}$ and $Pu^{V/VI}$. This suggests that these elements are potentially indistinguishable in the actual chemical processes occurring in aqueous carbonate solution systems, such as the nuclide migration in groundwater. Besides, a systemic comparison of $An^{V/VI}$ tricarbonato complexes has indicated that an increase in 5f electrons strengthens the $An-O_{ax}$ bonding, while it has almost no effect on the carbonate ligation. In a highly basic carbonate solution of 2.0 M Na_2CO_3/1.0 M NaOH with pH > 13, Np^V is electrochemically oxidized to Np^{VII} by undergoing a drastic structural rearrangement from the transdioxo tricarbonato complex to a square-planar-tetraoxo dihydroxo complex, $[Np^{VII}O_4(OH)_2]^{3-}$. This heptavalent Np is of great interest in the actinide chemistry, since we can hardly attain this highest oxidation state with other An.

Acknowledgment. We are thankful to K. Müller, K. Heim, and H. Foerstendorf (FZD−IRC) for the experimental support on ATR FT-IR measurement. All the DFT calculations in this study were carried out on the supercomputer at Zentrum für Informationsdienste und Hochleistungsrechnen (ZIH), Technische Universität Dresden (TUD), Germany. This work was supported by the Deutsche Forschungsgemeinschaft under Contract HE2297/2-1.

Supporting Information Available: UV−visible−NIR absorption spectra, structural drawing of neptunyl tricarbonato complex, a detailed description of the calculations of ionic radii, EXAFS spectra, calculated EXAFS structural parameters, coordinates and IR spectra of the DFT-optimized complexes, IR spectrum of Np^{VII} in 2.0 M Na_2CO_3/1.0 M NaOH. This material is available free of charge via the Internet at http://pubs.acs.org.